Received: 28 May 2019
DOI: 10.1002/mop.32499

WILEY

RESEARCH ARTICLE

Thermo-electro-optic energy conversion using plasmonic island embedded silicon microring circuit

Montree Bunruangses[1] | **Phichai Youplao**[2] | **Suphanchai Punthawanunt**[3] | **Iraj Sadegh Amiri**[4] | **Nithiroth Pornsuwancharoen**[5,6] | **Preecha Yupapin**[5,6]

[1]Department of Computer Engineering, Faculty of Industrial Education, Rajamangala University of Technology Phra Nakhon, Bangkok, Thailand

[2]Department of Electrical Engineering, Faculty of Industry and Technology, Rajamangala University of Technology Isan Sakon Nakhon Campus, Sakon Nakhon, Thailand

[3]Faculty of Science and Technology, Kasem Bundit University, Bangkok, Thailand

[4]Division of Materials Science and Engineering, Boston University, Boston, Massachusetts, USA

[5]Computational Optics Research Group, Advanced Institute of Materials Science, Ton Duc Thang University, District 7, Ho Chi Minh City, Vietnam

[6]Faculty of Applied Sciences, Ton Duc Thang University, District 7, Ho Chi Minh City, Vietnam

Correspondence
Preecha Yupapin, Faculty of Applied Sciences, Ton Duc Thang University, District 7, Ho Chi Minh City, Vietnam.
Email: preecha.yupapin@tdtu.edu.vn

Funding information
Rajamangala University of Technology Phra Nakhon

Abstract

We propose the use of the thermo-electro-optic energy conversion system for daily sunlight charger. A circuit consists of a modified silicon microring circuit embedded by a plasmonic island at the center. The island materials consist of silicon-graphene-gold layers. The thermal expansion of the island materials from the daily sunlight can affect the change in island material lengths and transfer to the plasmon wave path difference, which can perform the energy conversion and a charger. In manipulation, the daily sunlight statistic from South East Asia, the significant daily charging mobility of 4.34×10^{-6} cm^2. (V. s)$^{-1}$/Vs with the input light power of 10 mW can be obtained, which may be useful for one of the selected alternative energy sources.

KEYWORDS

microring circuit, microring resonator, plasmonic circuit, plasmonic island, thermo-electric circuit

1 | INTRODUCTION

Variant daily sunlight in nature is the powerful energy resource, which can be found in many applications,[1-5] especially for solar cell device input energy. However, the efficiency of such devices is still continuously improved.[6,7] There is another way of an application when the heat from sunlight can be used to form the thermal devices,[8,9] in which the direct thermal energy can be applied and the device functioned. Recently, the use of the variant sunlight for thermo-electric has shown a very interesting aspect, which can be used for an electrical device. In this article, we propose the use of the thermo-electro-optic energy conversion, in which the required output is the electron mobility that can be converted to be the required electrical output. By using the whispering gallery mode (WGM) output of the generated output beam, the reflected light intensity is given by $\boldsymbol{I_{WGMR} = -R_{WGM}\, I_{WGMR}}$. $\boldsymbol{R_{WGM}}$ is the reflection output. Here, $\boldsymbol{R_{WGM}}$, is a coefficient of the reflection or the used material reflectivity.[10]

2 | BACKGROUND

In the manipulation, the input electric field, $\boldsymbol{E_{in} = E_Z = E_0 e^{-ik_z - \omega t + \varphi}}$, is fed into the system along the z-axis direction with the wave propagation number $\boldsymbol{k_z}$. $\boldsymbol{E_0}$ represents the amplitude of the initial electric field, $\boldsymbol{\omega}$ and $\boldsymbol{\varphi}$ represent the angular frequency and the phase of the propagation light, respectively.[10]

$$\boldsymbol{E_{th} = \sqrt{1-\gamma_1}\left(\sqrt{1-\kappa_1}\,E_{in} + j\sqrt{\kappa_1}\,E_4\, e^{-\frac{\alpha L_p}{2\,4} - jk_n\frac{L_p}{4}}\right)} \quad (1)$$

$$\boldsymbol{E_{dr} = \sqrt{1-\gamma_3}\left(\sqrt{1-\kappa_3}\,E_{add} + j\sqrt{\kappa_3}\,E_2\, e^{-\frac{\alpha L_p}{2\,4} - jk_n\frac{L_p}{4}}\right)} \quad (2)$$

$$\boldsymbol{E_{out} = \sqrt{1-\gamma_3}\left(\sqrt{1-\kappa_3}\,E_{dr}^{*} + j\sqrt{\kappa_3}\,E_2\, e^{-\frac{\alpha L_p}{2\,4} - jk_n\frac{L_p}{4}}\right.} \quad (3)$$

$\boldsymbol{E_{dr}^{*} = -nE_{dr}}$, where $\boldsymbol{n}$ is the ratio of the reflection, E_{out} represents the output electrical field that appears at the add

port. Each the electrical field that propagates within each part of the system represents by E_1, E_2, E_3, E_4, E_L, and E_R, illustrated as in Figure 1. The intensity insertion loss coefficients are 3 dB couplers, which is represents by γ_{is}, and κ_{is} are the coupling coefficients. The attenuation loss due to light propagates within the waveguide is α. The propagation constant is $k_n = \frac{2\pi}{\lambda} n_{eff}$.

The circumference of the island ring circumference is L_D, which is changed under the change with the daily variant temperature. The change in the linear dimension can be estimated to be $\Delta L_D/L_D = \alpha_L \Delta T$, where ΔL_D is the change in the island ring circumference, α_L is the thermal expansion coefficient, ΔT is the change in temperature. However, the elongation limits of all materials are the applied conditions. The relation of the volume expansion coefficient as a function of the temperature can be evaluated by Grüneisen' s equation,[11] which can be express as Equations (4)-(8).[12]

$$\beta = \frac{1}{V}\left(\frac{\partial V}{\partial T}\right)_P \tag{4}$$

$$\beta = \frac{C_V}{Q_0[1-k(U/Q_0)]^2} \tag{5}$$

$$\frac{\Delta V}{V_0} = \beta \Delta T \tag{6}$$

where $\Delta V/V_0$ is the fractional change in volume, C_V is the capacity of molar heat considered at constant volume, U is

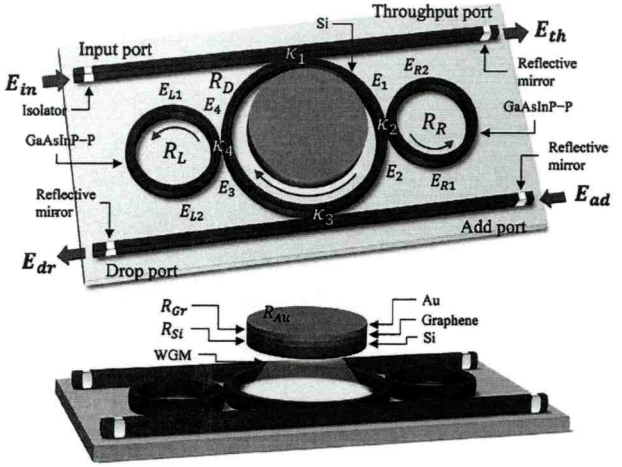

FIGURE 1 A microring circuit with the embedded plasmonic island at the centre ring, where R_L, R_R, R_D: the radius of the left, right, and centre ring, respectively. The coupling coefficients: $\kappa_s = 0.5$. R_{Au}, R_{Si}, R_{Gr}: the radius of Gold, Silicon, and Graphene plate, respectively. E_{in}, E_{th}, E_{dr}, and E_{ad}, represent the electrical fields of each port, throughput port, drop port, and add port, respectively [Color figure can be viewed at wileyonlinelibrary.com]

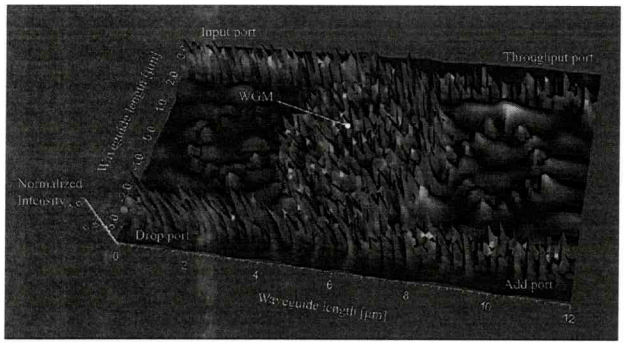

FIGURE 2 Graphical results obtained by the Optiwave program, where the used output is the whispering gallery mode (WGM) at the centre of the circuit as shown in Figure 1. The ring system, $R_L = R_R = 1.1$ μm, $R_D = 2.0$ μm, $\kappa_1 = \kappa_2 = \kappa_3 = \kappa_4 = 0.5$, $R_{Si} = R_{Au} = R_{Ga} = 1.6$ μm, of which the thickness: 0.1 μm, 0.1 μm, and 0.2 μm, respectively, $n_{Si} = 3.47$. The input power is 10 mW with 1.55 μm center wavelength [Color figure can be viewed at wileyonlinelibrary.com]

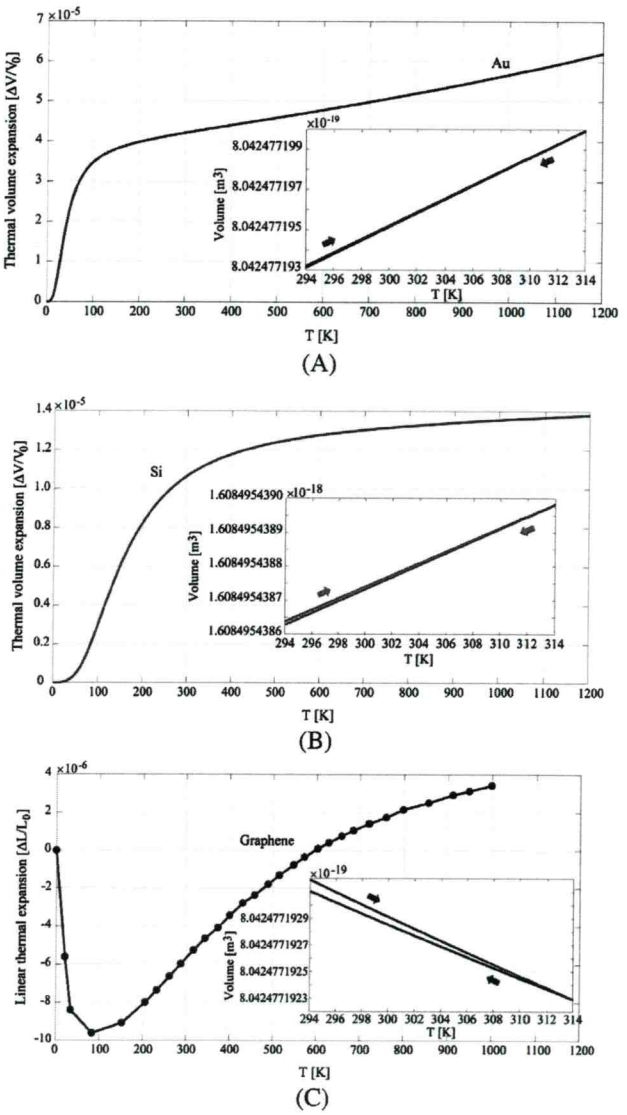

FIGURE 3 Thermal expansion of the island rings-silicon, graphene, gold, where A, and B,[11] C[12,13] [Color figure can be viewed at wileyonlinelibrary.com]

TABLE 1 Specified parameters for charge-carrier number density evaluation[16]

	Density (g/cm^3)	Free electron number	Molar mass (g/mol)	Conductivity: σ (S/m)
Au	19.30	1	196.97	4.10×10^7

the lattice vibrations energy, Q_0 and k are constant quantities. Then, with a specified Debye temperature, θ_D, both C_V and U at any temperature T can be calculated by using Equations (7) and (8), where R is the molar gas constant.

$$C_V = 3R\left[12\left(\frac{T}{\theta_D}\right)^3\int_0^{\theta_D/T}\frac{x^3dx}{e^x-1} - 3\frac{\theta_D/T}{e^{\theta_D/T}-1}\right] \quad (7)$$

$$U = \int_0^T C_V\,dT \quad (8)$$

3 | SIMULATION RESULTS

By using the graphical program called an Optiwave program, from which the result of the WGM is obtained as shown in Figure 2, where the selected parameters of the system in Figure 1 were applied. The major role was the side ring radii that can be used to control to obtain the WGM output. From which the key effect was the nonlinear Kerr effect of the GaAsInP-P material. Those identified parameters will use for the MATLAB program later on. The used materials thermal characteristics are also are given in Figure 3, in which the fractional change in volume for Au and Si can be illustrated as in Figure 3A,B. In addition, for graphene, the fractional change in length can be considered from the theoretical data by References 13 and 14 and illustrated in Figure 3C. Based on the average temperature, according to statistics such as Bangkok, Thailand, which changes in the range of 20°C to 40°C (~294°K-314°Kelvin),[15] the volume change of the island according to the type of material can be considered as follows. Figure diagram in each figure of Figure 3. The parameters are given by the following details. As the specified parameters used in Table 1, the charge-carrier number density for an Au island can be calculated by an Equation (8), which is $\boldsymbol{n} = 5.8987 \times 10^{28}$ electrons.$\boldsymbol{m}^{-3}$. The Au island radius $R_{Au} = 1.6$ μm, of which the thickness is 100 nm. Then the calculated charge-carrier is 4.7440×10^{10} electrons, where an electron charge, $e = 1.602 \times 10^{-19}$ coulombs. Thus, the island's maximum electrical charge is $Q_{max} = 7.5999 \times 10^{-9}$ coulombs. Furthermore, the current density, $J = \sigma E$, where E represents the electric field inside the Au plate and its conductivity (σ) are related to the thickness of the plate (T_{Au}). The cross-sectional area of the Au island is $A = \pi[R_{Au}]^2$. Thus, the charging current can be considered as $I = JA = \sigma T_{Au} EA$ and results in the induced charge Q within the Au plate, which can be expressed by a function of time: t, as $Q = I \times t$. Therefore, the time-dependent charge on the Au plate within the plasmonic island can be expressed by $Q(t) = [\sigma T_{Au} EA \times t]$. This time-dependent charging Q can be illustrated as shown in Figure 4A, in which the discharging state will depend on the applied loads. For simplification, it starts from the maximum charge, Q_{max}, on the plasmonic island and the load draws the current as an electrons source, an amount of electrons/s (Q/s). Thus, the time-dependent discharging Q can be considered as $Q(t) = [Q_{max} - met]$, which is illustrated in Figure 4B, where m is an amount of discharging in electrons/s. The daily sunlight with the charging current is shown in Figure 5A, which can have the electron mobility within the operation period as shown in Figure 5B. The electron mobility can be changed to the electrical current and found in the Reference 18.

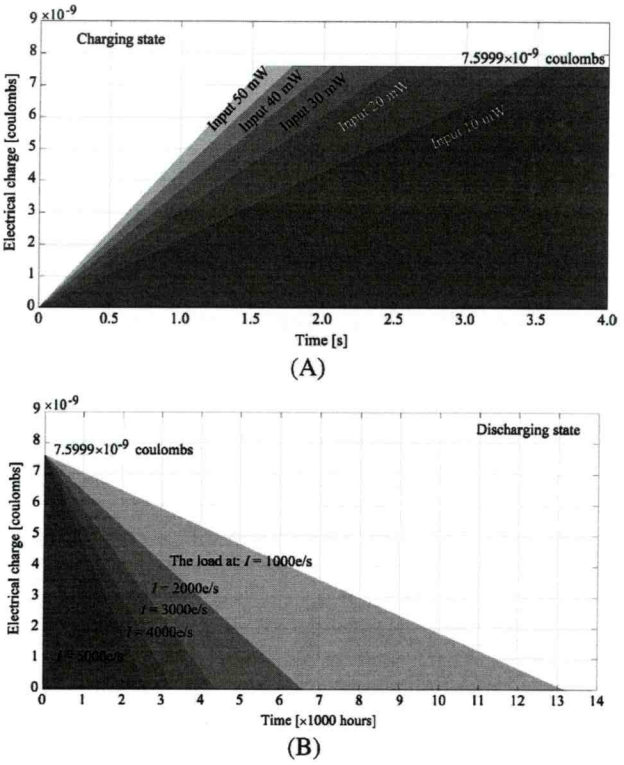

FIGURE 4 Results of the induced electrical charge characteristics using the proposed circuit, A, the charging state, where the input light powers are varied from 10 to 50 mW, and B, the discharging state, where the loads are varied from 1000 to 5000 e/s [Color figure can be viewed at wileyonlinelibrary.com]

4 | CONCLUSION

The proposed micro-circuit for the thermo-electro-optic energy conversion is a very interesting device that can be

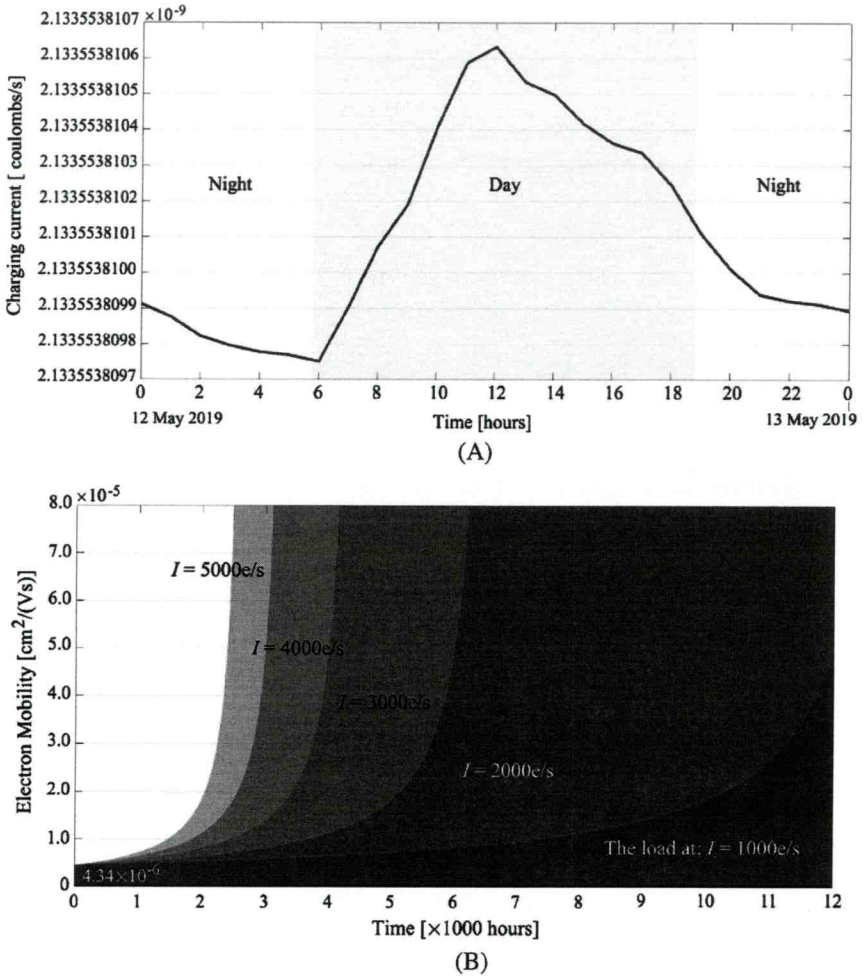

FIGURE 5 In manipulation, the thermal expansion is employed by the relationship between the input light power and the induced electron mobility, where A, the reference to a weather data record,[17] B, the daily charging current for the input light power of 10 mW can be obtained as in the figure, from which the electron mobility of 4.34×10^{-6} cm^2. $(V. s)^{-1}$ can be obtained [Color figure can be viewed at wileyonlinelibrary.com]

practically fabricated and used as one of the selected alternative energy sources. In the manipulation, the significant result of the daily charging electron mobility of 4.34×10^{-6} cm^2.$(V. s)^{-1}$ with the input light power of 10 mW can be obtained. The large area circuits can also be employed to achieve more mobility output for further applications.

ACKNOWLEDGMENT

The authors would like to give the appreciation for the research financial support from Rajamangala University of Technology Phra Nakhon, Bangkok, 10300, Thailand.

ORCID

Iraj Sadegh Amiri https://orcid.org/0000-0001-8121-012X

Preecha Yupapin https://orcid.org/0000-0002-6438-9276

REFERENCES

[1] Mitatha S, Kamoldilok S, Yupapin PP. White light generation and amplification using a soliton pulse within a nano-waveguide for potential of solar energy conversion use. *Energ Conver Manage*. 2010;51:2340-2344.

[2] Kamoldilok S, Yupapin PP. Nanoheat source generated by leaky light mode within a nano-waveguide for small electrical generator. *Energ Conver Manage*. 2012;64:23-27.

[3] Srithanachai I, Uemmanapong S, Niemcharoen S, Yupapin PP. Novel design of solar cell efficiency improvement using an embedded electron accelerator on-chip. *Opt Express*. 2012;20:12640-12648.

[4] Ali J, Pornsuwancharoen N, Youplao P, et al. Coherent light squeezing states within a modified microring system. *Results Phys*. 2018;9:211-214.

[5] Pornsuwancharoen N, Amiri IS, Suhailin FH, et al. Micro-current source generated by a WGM of light within a stacked silicon-graphene-Au waveguide. *IEEE Photon Technol Lett*. 2017;29:1768-1771.

[6] Sasihithlu K, Dahan N, Greffet JJ. Light trapping in ultrathin CIGS solar cell with absorber thickness of 0.1 μm. *IEEE J Photovolt*. 2018;8:621-625.

[7] Gupta ND, Janyani V. Lambertian and photonic light trapping analysis with thickness for GaAs solar cells based on 2D pereodic pattern. *IET Optoelectron*. 2017;11:217-224.

[8] Goffard J, Colin C, Mollica F, et al. Light trapping in ultrathin CIGS solar cells with nanostructured back mirrors. *IEEE J Photovolt*. 2017;7:1433-1441.

[9] Gupta ND, Janyani V. Design and analysis of light trapping in thin film GaAs solar cells using 2-D photonic crystal structures at front surface. *IEEE J Quantum Electron*. 2017;53: 4800109.

[10] Chaiwong K, Tamee T, Punthawanunt S, et al. Naked-eye 3D imaging model using the embedded micro-conjugate mirrors within the medical micro-needle device. *Microsyst Technol*. 2018; 24:2695-2699.

[11] Graham MG, Hagy HE. *Thermal Expansion*. NewYork: American Institute of Physics; 1971:1972.

[12] Zhang B, Li X, Li D. Assessment of thermal expansion coefficient for pure metals. *CALPHAD*. 2013;43:7-17.

[13] Jiang JW, Wang JS, Li B. Young's modulus of graphene: a molecular dynamics study. *Phys Rev B*. 2009;80:205429.

[14] Mann S, Kumara R, Jindal VK. Negative thermal expansion of pure and doped graphene. *RSC Adv*. 2017;7:22378-22387.

[15] "Climatological Data for the Period 1981–2010." Thai Meteorological Department. Accessed September 2, 2016:16-17.

[16] Serway RA. *Principles of Physics*. 2nd ed. Fort Worth, TX: Saunders College Publishing; 1998 p. 602.

[17] Meteoblue. Weather history download Bangkok. *Meteoblue*. www.meteoblue.com/en/weather/archive/export/bangkok_thailand_1609350. Accessed May 18, 2019.

[18] Ali J, Youplao P, Pornsuwancharoen N, et al. Nano-capacitor-like model using light trapping in plasmonic island embedded microring system. *Results Phys*. 2018;10:727-730.

How to cite this article: Bunruangses M, Youplao P, Punthawanunt S, Amiri IS, Pornsuwancharoen N, Yupapin P. Thermo-electro-optic energy conversion using plasmonic island embedded silicon microring circuit. *Microw Opt Technol Lett*. 2020;1–5. https://doi.org/10.1002/mop.32499

MICROWAVE AND OPTICAL TECHNOLOGY LETTERS

Edited By: Wenquan Che

Impact factor: 0.957

2019 Journal Citation Reports (Clarivate Analytics): 220/266 (Engineering, Electrical & Electronic) 80/97 (Optics)

Online ISSN: 1098-2760

About This Journal

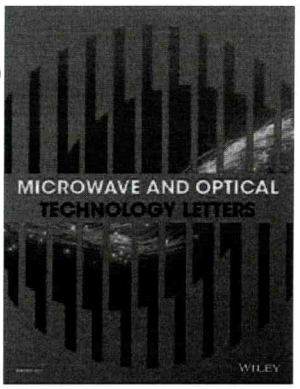

Microwave and Optical Technology Letters provides quick publication (3 to 6 month turnaround) of the most recent findings and achievements in high frequency technology, from RF to optical spectrum. The journal publishes original short papers and letters on theoretical, applied, and system results in RF, Microwave, and Millimeter Waves, Antennas and Propagation, Submillimeter-Wave and Infrared Technology, and Optical Engineering.

Read the journal's full aims and scope.

Articles

Most Recent

Free Access

Erratum

MICROWAVE AND OPTICAL TECHNOLOGY LETTERS

Early View

Online Version of Record before inclusion in an issue

Export Citation(s)

Erratum

Free Access

Erratum

Version of Record online: 22 July 2020

https://doi.org/10.1002/mop.32559

This article corrects the following: >

Full text | PDF | Request permissions

RESEARCH ARTICLES

Full Access

A new class of wideband microstrip falcate patch antennas with reconfigurable capability at circular-polarization

https://doi.org/10.1002/mop.32514

Abstract | Full text | PDF | References | Request permissions

Full Access

New design of an adjustable compact microstrip lowpass filter using Z-shaped resonators with low VSWR

Mahmoud Alizadeh Pahlavani, Masoud Moradkhani, Ramin Sayadi

Version of Record online: 22 June 2020

https://doi.org/10.1002/mop.32503

Abstract | Full text | PDF | References | Request permissions

Full Access

A miniaturized electromagnetically coupled patch antenna design using eroded ground plane

Amiya Bhusana Sahoo, Biswa Binayak Mangaraj

Version of Record online: 20 June 2020

https://doi.org/10.1002/mop.32480

Abstract | Full text | PDF | References | Request permissions

Full Access

Compact K/Ka-band dipole antenna element with ball grid array packaging

Xiubo Liu, Wei Zhang, Dongning Hao, Yanyan Liu

Version of Record online: 20 June 2020

https://doi.org/10.1002/mop.32510

Abstract | Full text | PDF | References | Request permissions

Full Access

A 24 GHz hydrology radar system capable of wide-range surface velocity detection for water resource management applications

Yo-Sheng Lin, Shang-Feng Chiu, Chi-Ho Chang

Version of Record online: 19 June 2020

https://doi.org/10.1002/mop.32479

Jiachen Guo, Jia Bo, Huang Tang, Dong Zhao, Pengwei Zhou, Jian Wang

Version of Record online: 18 June 2020

https://doi.org/10.1002/mop.32471

Abstract | Full text | PDF | References | Request permissions

Full Access

Analysis of via-fed cylindrical dielectric resonator antennas

Juner M. Vieira, Marcos V. T. Heckler

Version of Record online: 18 June 2020

https://doi.org/10.1002/mop.32513

Abstract | Full text | PDF | References | Request permissions

Full Access

Thermo-electro-optic energy conversion using plasmonic island embedded silicon microring circuit

Montree Bunruangses, Phichai Youplao, Suphanchai Punthawanunt, Iraj Sadegh Amiri, Nithiroth Pornsuwancharoen, Preecha Yupapin

Version of Record online: 18 June 2020

https://doi.org/10.1002/mop.32499

Abstract | Full text | PDF | References | Request permissions

Full Access

Electron cloud spin generated by microring space-time control circuit for 3D quantum printing

Arumona Edward Arumona, Suphanchai Punthawanunt, Kanad Ray, Sirigiet Phunklang, Preecha Yupapin

Version of Record online: 18 June 2020

https://doi.org/10.1002/mop.32490

Abstract | Full text | PDF | References | Request permissions